Enhancing Plasma Density through Periodic Dielectric Grating Structures-Numerical Simulations

David Kakulia[1], Kakhaber Tavzarashvili[2], Irakli Noselidze[2], Giorgi Kajaia[2]

[1]Department of Electrical and Electronics Engineering, Faculty of Exact and Natural Sciences, Iv. Javakhishvili Tbilisi State University, 0179 Tbilisi, Georgia

[2]School of Science and Technology, The University of Georgia, 0171 Tbilisi Georgia

Corresponding author: Irakli Noselidze (e-mail ira.noselirdze@ug.edu.ge).

ABSTRACT This paper proposes an idea of the use of Dielectric Resonators (DRs) as concentrators of alternating magnetic fields for plasma density control applications. The study involves numerical simulations using the Method of Auxiliary Sources (MAS) to analyze Dielectric Frequency Selective Surfaces (DFSS) composed of periodic dielectric elements. Materials with variable dielectric permittivities, including E-Glass, Plexiglass, Taconic CER-10, and Teflon are considered, and their resonance properties are investigated. Results indicate that DFSSs can create strong magnetic fields at resonance frequencies, which can be utilized for plasma density regulation in processes like thin film deposition. The results demonstrate that materials with lower dielectric permittivity, such as Plexiglass and Teflon, exhibit higher resonance quality factors, while higher permittivity materials like E-Glass and Taconic CER-10 show poorer quality factors. The study emphasizes the potential of DFSSs in enhancing plasma density and improving industrial applications, highlighting the importance of precise geometric configurations and material properties in designing effective dielectric resonators.

INDEX TERMS Dielectric Resonators, Frequency Selective Surfaces, Plasma, Numerical Methods.

I. INTRODUCTION

In this paper Dielectric resonator (DR) is considered as "concentrator" of alternating magnetic field for plasma density control applications. Generally, DRs are passive components widely used in microwave and millimeter-wave applications for their high-quality factor (Q-factor) and low loss characteristics. DRs operate based on the principle of dielectric resonance, in which electromagnetic waves are confined within a specific region inside or outside the dielectric with a high permittivity. The resonant frequency of a dielectric resonator depends on its physical dimensions, the dielectric constant of the material, and the mode of resonance. Resonance fields are very strong for both electric and magnetic fields. Great interest in DRs is also caused by their high frequency stability and low phase noise. These features are essential in applications such as radar systems, communication transmitters, and local oscillators in receivers. DR filters provide high selectivity and low insertion loss, making them ideal for use in bandpass and bandstop filters. Despite their advantages, DRs face several challenges. One major challenge is the precise fabrication required to achieve the desired resonant frequencies, especially at high frequencies. It is important to propose DRs with a shape suitable for fabrication, investigate tolerance of their properties relative to geometric inaccuracy.

Advances in material science and computational modeling continue to drive the development of more efficient DRs. As technology progresses, DRs are expected to play an increasingly important role in the advancement of systems and will find broader application.

The important examples of structures with high-quality factor (Q-factor) and strong resonance properties are the Frequency Selective Surfaces (FSS) [1, 2, 3]. They are engineered structures that exhibit selective frequency filtering properties, allowing certain frequencies to pass while blocking others. They find applications across various fields such as telecommunications, radar, and electromagnetic compatibility. Usually, FSS are composed of periodic arrays of conductive elements on a dielectric substrate. The behavior of these surfaces is governed by their geometry, material properties, and the arrangement of the elements. By carefully designing these parameters, FSS can be tailored to exhibit band-pass, band-stop, high-pass, or low-pass filtering characteristics.

One special group of FSS is Dielectric Frequency Selective Surfaces (DFSS). They are comprised of periodic arrays of dielectric elements that can control the propagation of electromagnetic waves through selective frequency filtering. Unlike traditional metallic FSS, DFSS rely on dielectric materials to achieve their frequency selective properties. These surfaces leverage the interaction between the electromagnetic waves and the dielectric materials' intrinsic properties, such as permittivity, and geometric configuration as well.

The interaction of electromagnetic waves with FSS results in constructive and destructive interference patterns, which define the transmission and reflection properties at different frequencies. The key parameters influencing the performance include the size, shape, and spacing of the elements, as well as the dielectric constant of the substrate. It is worth noting that for certain combinations of surface geometry, incidence angles, wavelengths, and material characteristics, anomalous behavior in diffraction and refraction can be observed. These effects are utilized in many practical applications [4, 5].

Designing DFSS with desired features of applicability requires sophisticated computational tools and techniques [6, 7, 8, 9]. The following methods are commonly used:

- Finite-Difference Time-Domain (FDTD): This method is effective for time-domain simulations and can model the interaction of electromagnetic waves with complex dielectric structures.
- Finite Element Method (FEM): the FEM is used for solving complex geometries and material properties, providing detailed insights into the electromagnetic field distribution.
- Method of Moments (MoM): the MoM is suitable for frequency-domain analysis and is used to solve surface integral equations, especially in planar structures.
- Method of Auxiliary Sources: the MAS is effective for frequency domain simulations and can model interaction with homogenous dielectric structures with complex, smooth shapes.

The design process involves selecting available, appropriate, dielectric materials with desired permittivity and loss tangent values. Common materials include ceramics, polymers, and composites with high dielectric constants. The geometric configuration of the dielectric elements, such as their shape, size, and spacing, plays a crucial role in determining the DFSS performance.

It is expected that DFSS can create strong magnetic field at resonance frequency. The magnetic field can be controlled by electromagnetic waves source intensity. This phenomenon that can be used to control plasma density, becomes a kind of plasma manipulation instrument [10,11,12].

In many applications enhancing plasma density in specific regions is crucial. An essential example is magnetron, where higher plasma densities lead to higher ionization rates inside the magnetron chamber, resulting in increased ion flux towards the target surface. This, in turn, enhances the sputtering yield and deposition rate, crucial for various industrial applications such as semiconductor manufacturing, optical coatings, and thin film solar cells. Additionally, increased plasma density can improve film properties such as density, adhesion, and uniformity.

The primary objective of the present study is to explore the influence of different grating shapes and materials on formation magnetic field at resonance frequency. This includes investigation of various geometric parameters such as: grating period, shape of boundaries, as well as different dielectric materials. The paper is structured by following way: Section 2 addresses to the Method of Auxiliary Sources. The periodic green function is constructed(derived) for solving 2D problems with p-polarization and periodic dielectric structures of arbitrary shape. Section 3 describes geometries and materials of the considered periodic dielectric structures. In the Section 4 results of numerical simulation are presented. Section 5 contains conclusions.

II. THE METHOD OF AUXILIARY SOURCES

The MAS is a numerical technique used to solve boundary problems in static cases or when the time factor is harmonic. V. Kupradze formulated the foundational principles of this method, setting it apart from the integral equation method [13]. The integral formulation of the MAS is based on the concept of an auxiliary contour or surface (hereafter referred to as contour). V. Kupradze provided proof of the completeness and linear independence of the series of fundamental solutions, with poles distributed over a closed auxiliary contour.

In the MAS, the fundamental solutions correspond to either the Helmholtz or Laplace equations, depending on the problem. For example, in the case of a single object, the scatterer's boundary contour divides space into two areas physically not connected to each other. Auxiliary contours are defined for each area in its non-physical counterpart [14,15]. For a dielectric object, two auxiliary contours are needed: one for the outer area and one for the inner area. In the case of a perfectly or highly conductive object, to express scattered field one auxiliary contour is sufficient.

The approximate solution in the MAS is represented by a finite series of fundamental solutions (e.g., Green functions) [16]. The coefficients of the series elements are calculated to satisfy the boundary conditions. For this the system of linear equations should be solved. The number of linear equations, i.e. the number of unknowns, depends on particular case: wavelength, incidence angle, surface geometry etc. Convergence of the solution is achieved similarly to the Method of Moments (MoM) [17,18,19], by repeatedly solving the problem with an increasing number of series elements until the accuracy becomes acceptable. The MAS circumvents the singularity problems typical of MoM or the Integral Equation Method, allowing for the evaluation of boundary condition fulfillment and the assessment of solution accuracy.

As mentioned above, the aim is to investigate the DFSS numerically. The MAS should be formulated for 2D spatially periodic problems with p-polarization [20].

For convenience, the harmonic $e^{-i\omega t}$time factor is chosen and omitted in further expressions. Mathematically, there is no preference between $e^{-i\omega t}$and $e^{i\omega t}$ time factors. This is just a small remark for computation. When calculating wave number of a medium with complex permittivity and permeability, calculation should be done using the formula $k = k_0\sqrt{\varepsilon}\sqrt{\mu}$ [21], where k is the wave number in medium, k_0 is the wave number in free space; ε and μ are the permittivity and permeability of the medium. Therefore, to obtain physically meaningful results, the order of operations matters: take the square roots first $\sqrt{\varepsilon}\sqrt{\mu}$, and then perform the multiplication.

The problem can be reduced to 2D when the field is homogenous in one direction [22]. The electric vector potential field $\vec{F}_M$ produced by periodic monopole sources distributed along x axis is given by following sums:

$$\vec{F}_M(x,y) = \frac{i\varepsilon_0\varepsilon_r\vec{I}}{4} = \sum_{n=-\infty}^{\infty}\exp(\,i\Delta\phi n)H_0^{(1)}(kr) \qquad (1)$$

$$r = \sqrt{(x-nd-x')^2+(y-y')^2}$$

Here $\vec{I}_M = (0,0,1)$ specifies direction of magnetic current; x', y' are coordinates of the n=0 monopole; x, y - are coordinates of the observation point; k is the wave number in this medium; ε_r is relative permittivity of the medium; ε_0 is electric constant; $H_0^{(1)}$ is zeroth order Hankel's function of first kind; d stands for a period of array of monopoles along in x-direction; $\Delta\phi$ is the phase shift. Sum (1) converges very slowly.

In general, the Poisson summation formula

$$\sum_{p=-\infty}^{\infty} g(p) = \sum_{q=-\infty}^{\infty} f(\,2\pi q)$$

where,

$$g(p) = \int_{-\infty}^{\infty} e^{-jpt}f(t)dt$$

is applied to (1) that gives following sum:

$$\vec{F}_M(x,z) = \frac{\varepsilon_0\varepsilon_r\vec{I}_M}{2d}\sum_{n=-\infty}^{\infty}\frac{exp(i\vec{\rho}\cdot\vec{k}^n)}{k_y^n} \qquad (2)$$

Where $\vec{\rho} = (x-x', y-y', 0)$, $\vec{k}^n = (k_x^n, k_y^n, 0)$ is complex vector, with components

$$k_x^n = \frac{\Delta\phi+2\pi n}{d}, k_y^n = sign(y-y')\sqrt{k^2-(k_x^n)^2}$$

Only first root of $\sqrt{k^2-(k_x^n)^2}$ is applicable. k_z^n depends on sign$(y-y')$ indicating that space "cut" exists on $y = y'$ plane. It is easy to note, for any k, such m exists, when $|n| > m$, $k^2-(k_x^n)^2 < 0$. Considering this, for $\rho_y \neq 0$, the sum (2) converges like

$$\sum_{n=1}^{\infty}\frac{exp(-n)}{n}$$

However, if $\rho_y = 0$, there is no convergence, like the sum $\sum_{n=1}^{\infty}\frac{1}{n}$ [23].

Expressing

$$\vec{H} = i\omega\vec{F}_M \; and \; \vec{E} = -\frac{1}{\varepsilon_0\varepsilon_r}\vec{\nabla}\times\vec{F}_M$$

where ω is angular frequency, one obtains:

$$H_x = 0, H_y = 0, H_z = \frac{\omega\varepsilon_0\varepsilon_r}{2d}\sum_{n=-\infty}^{\infty}\frac{exp(i\vec{\rho}\cdot\vec{k}^n)}{k_z^n} \qquad (3)$$

and

$$E_x = \frac{1}{2d}\sum_{n=-\infty}^{\infty} exp(\,i\vec{\rho}\cdot\vec{k}^n), \text{ and}$$

$$E_y = \frac{1}{2d}\sum_{n=-\infty}^{\infty} k_x^n\frac{exp(i\vec{\rho}\cdot\vec{k}^n)}{k_y^n}, E_z = 0 \qquad (4)$$

E_y converges as (2), H_z converges like $\sum_{n=-\infty}^{\infty} exp(-|n|)$, when $\rho_y \neq 0$.

Other details of solving boundary problems by the MAS can be found in [24]. Results presented in [25] were taken as benchmark problems in [24].

III. FSS GEOMETRY AND MATERIALS

For numerical experiments, we consider dielectric layers with a periodic profile shown in the Figure 1. The shape repeats infinitely in the horizontal direction, creating a periodic structure. The geometric parameters of the periodic structure are presented in the Figure 1 down panels.

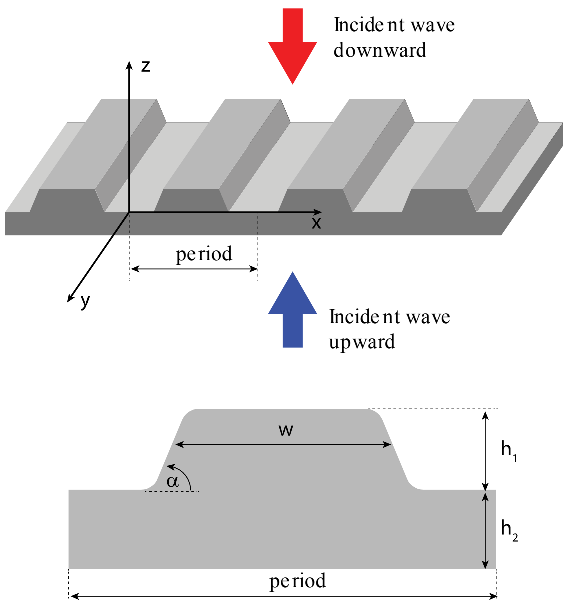

FIGURE 1. Geometry of DFSS.

Several parameters determine the grating configuration: lattice period, w - mid-width of the "hump", h_1 - height of the "hump", h_2 - thickness of the base layer, and angle α - the "hump" slope angle. Parameters w, h_1, h_1 are fixed; They are presented as unitless values, measured in units of the period. Specifically, w=0.5, h_1=0.3, h_2=0.3. It is important to note that the shape is not composed of straight lines; instead, it is curved at the joints with a radius of curvature of 0.3. This design choice is made to accommodate the MAS, which is less efficient when dealing with sharp angles or edges in geometric objects. The method generally produces stable results when the distance between the real and auxiliary contours is less than the radius of curvature. As this distance decreases, the efficiency of the method also decreases.

Three different types of geometries were considered where α takes the following values: 70°, 95°, and 110° shown on the Figure. 2. Calculations were done for many different angles between 70° and 110°. Only the major results are presented below.

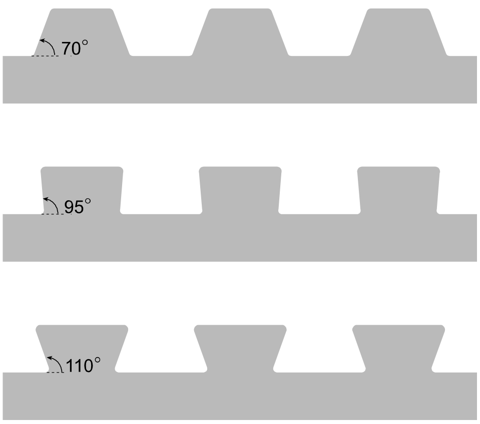

FIGURE 2. The angle α takes the following values: 70°, 95°, and 110°, which correspond to the geometry profile presented in the picture

These variations aim to investigate the tolerance of resonance frequencies to fabrication accuracy.

The proposed Dielectric Frequency Selective Surfaces (DFSS) are considered for various dielectric materials. The chosen dielectric materials are E-Glass, Plexiglass, Taconic CER-10, and Teflon. The relative dielectric permittivity of these materials is as follows: 6.22 for E-Glass, 2.59 for Plexiglass, 10.0 for Taconic CER-10, and 2.1 for Teflon.

IV. NUMERICAL RESULTS

Based on the above formulations, a FORTRAN computational code implementing the MAS has been developed and used in numerical experiments. To validate used method, we resort to benchmarking data of [26]. The work provides a relevant reference, presenting numerical results related to a periodic dielectric grating structure. Particularly, in [26] the effect of periodicity on plasmon-assisted scattering and absorption of visible light by infinite and finite gratings of circular silver nanowires is studied (Figure 3).

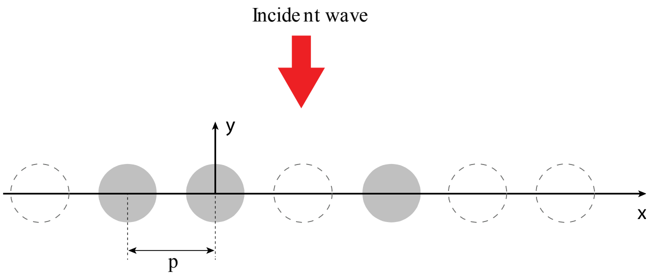

FIGURE 3. Infinite periodic grating of circular cylinders illuminated by a normally incident plane wave. Geometry concepts discussed in source [24].

The Figure 4 shows that the present method for the periodic grating with circular cylinders gives results that are in good agreement with those of [26]. We note that the comparison is made for E-Glass.

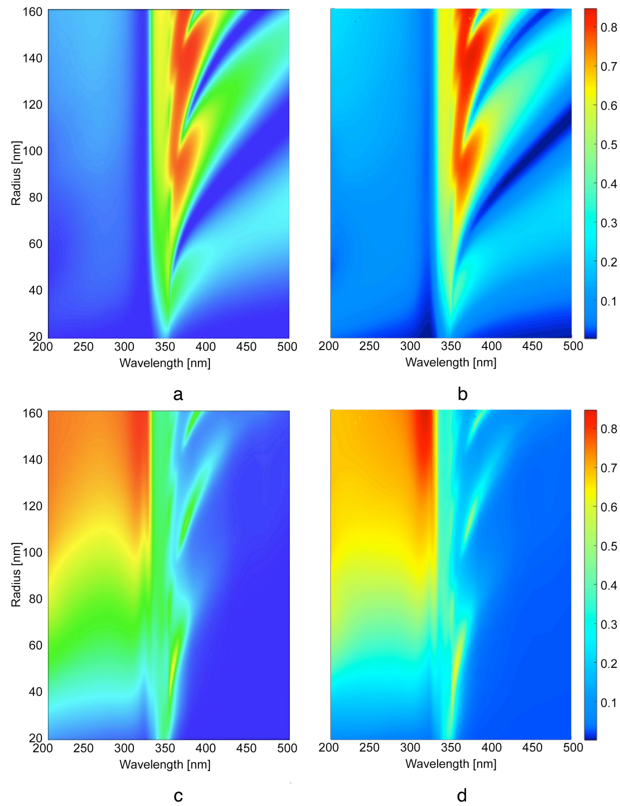

FIGURE 4. Demonstration of the MAS codes benchmarking [26]. Reflectance (top panels) and absorbance (down panels) of infinite grating of silver wires as a function of the wavelength and wire radius for the normal incidence of the H-polarized plane wave. The period is p = 350 nm. The pictures on the left side, a and c, were taken from reference [26], and the pictures on the right side, b and d are calculated using the MAS.

Diffraction on cylindrical surfaces is considered in [27, 28], where the critical radius for the auxiliary contour is determined. In the present study, the incident field is a plane wave, indicating that the source is infinitely far away. Additionally, the junctions of the flat areas of the contour are approximated by small-radius (0.03 - in period units) arcs. Considering these two factors, the critical radii become infinitely small, and thus the auxiliary contours naturally envelope conjugate points, as the auxiliary contours are separated from the real ones by half the radius. Consequently, oscillations in the distribution of auxiliary sources (currents) do not occur.

It is important to demonstrate the convergence of solutions. Numerical calculations demonstrate that convergence is achieved when number of linear equations is nearly 200 per unit of wavelength.

The Figure 5 a) shows the magnetic field values calculated at the test point (0,0.15,0) (in period units) over a wavelength/period range of [0.3,3]. Calculations are performed for $\alpha=85^0$ and with different numbers of unknowns: 300, 350, and 450.

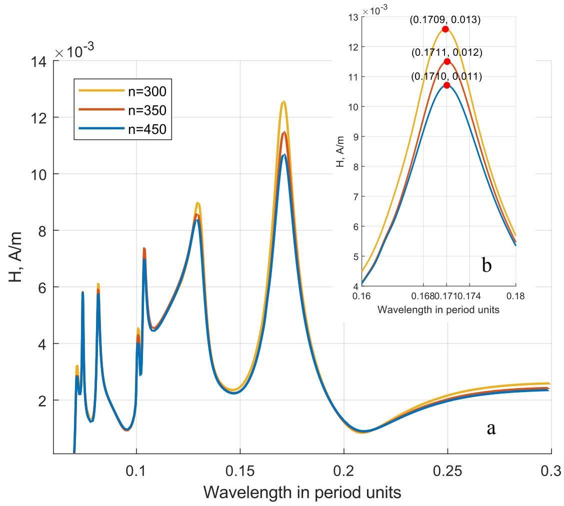

FIGURE 5. Curves of magnetic field dependences on wavelength for solutions with different numbers of unknows n. Zoomed-in plot of the Figure 5a graph, near the resonance point.

The figure illustrates that the developed code can obtain stable results. The Figure 5 b) shows a zoomed-in plot near the resonance point. As one can see, the accuracy of finding the resonance frequency is about 0.5%, while the accuracy of determining the peak value is 10%. This discrepancy represents the largest difference observed in the results. As the geometric sizes are presented as unitless values, it is reasonable to use unitless values for wavelengths too.

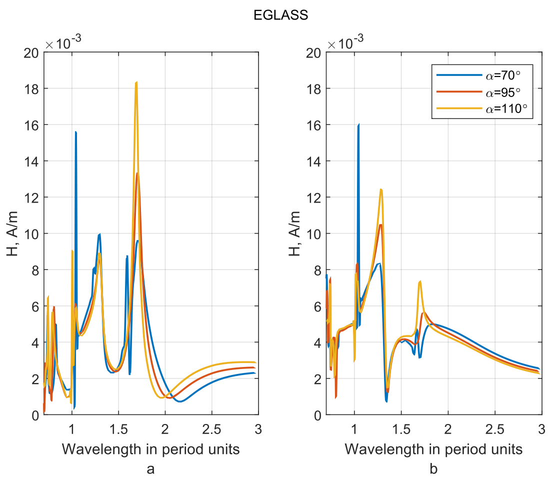

FIGURE 6. Magnetic fields in the test point, E-Glass case. a) incident wave downward, b) incident wave upward

All following results, as in previous cases, are obtained in the same wavelength range and relate to an incident plane wave with p-polarization, presenting absolute value the magnetic field. Two directions of unit amplitude plane wave incidence are considered: one vertically downward and the other vertically upward.

The Figure 6 shows magnetic field in the test point, when a plane wave with downward and upward direction incidents on the DFSS made of E Glass material. Results are obtained for different values of α.

It can be noted that in all cases, the magnetic field extremum at 1.7 (Figure 6 a) remains at the same location, although its value changes. This extremum with highest wavelength corresponds to the first resonance in a frequency range. This stability, despite variations in geometry, is important for fabrication. The lowest resonance frequency can find its application in the regulation of plasma density.

Let consider results for the same DFSSs when the incident plane wave has upward direction. Corresponding results are presented at the Figure 6b. In the upward cases, local extrema of the magnetic field at a wavelength of 1.7 still occur. They have changed character and become weaker compared to the downward cases. It is important to note that the resonance exposes itself while the DFSS acts as a shield for the test point.

Apparently, if we choose periodic grating for both sides of DFSS, then the resonance filed distribution would be symmetric, reflecting the geometry, and providing stronger fields. However, demonstrating asymmetric results is more informative.

The next case involves Plexiglass material. As shown in the Figure 7, the highest wavelength resonance occurs at 1.25 (Figure 7a). This resonance is very strong and stable for all cases compared to the E-Glass cases. It exhibits an eye-catching quality factor. Since the permittivity of Plexiglass is lower than that of E-Glass, the resonance occurs at a lower value of wavelength.

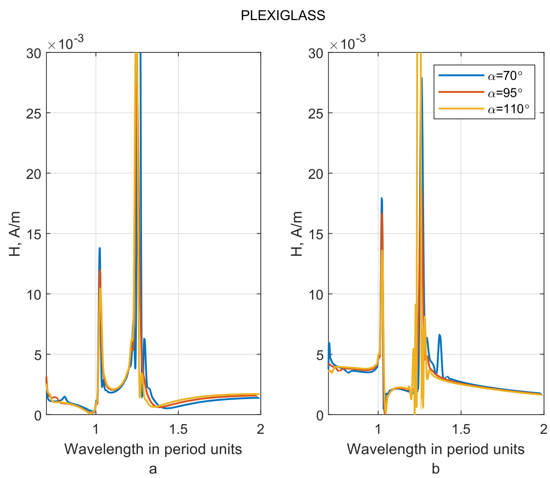

FIGURE 7. Magnetic fields in the test point, Plexiglass case. a) incident wave direction is downward, b) incident wave direction is upward

The Figure 8 presents results related to Taconic CER-10 material. This material has the highest dielectric permittivity between considered materials. As it was expected it has local extremum at 2.054 of wavelength, which is greater than that E

Glass has. The Figures 8 a) and b) show relatively stable location of "resonance frequency". The quality factor looks pitiful. The Figure 8a) shows some complexity, while The Figure 8b) shows a local minimum of the magnetic field. The shielding effect of the Taconic CER-10 DFSS is strongly exhibited.

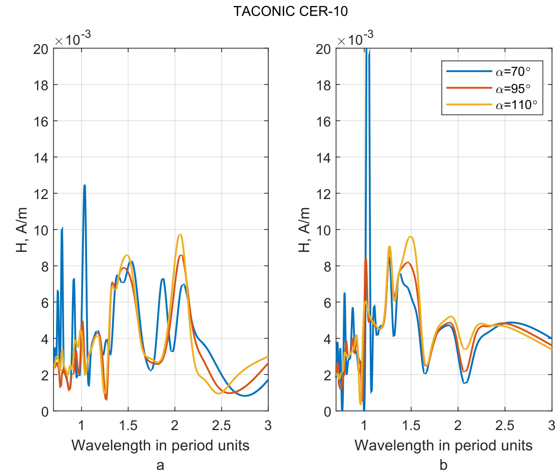

FIGURE 8. Magnetic fields in the test point, Taconic CER-10 case. a) incident wave downward, b) incident wave upward

The structure demonstrates resonance at the highest wavelength among the other DFSS. Its potential for application in the regulation of plasma density is promising. It is important to see how looks the resonance field distribution at 2.054 wavelength.

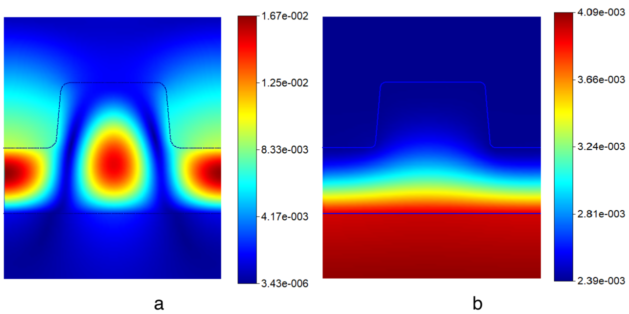

FIGURE 9. The Magnetic field distribution at 2.054 wavelength, incident wave downward (a) and upward (b), Taconic CER-10, α=85⁰ case

The Figure 9 shows the magnetic field distribution at a wavelength of 2.054. The pulse-shaped profile has $\alpha=85^0$. The material is Taconic CER-10, and the plane wave is incident in the downward direction. The magnetic field distribution exhibits a distinct resonant field shape, which stands out against the plane wave background. Sizes of the field distribution are presented also unitless in period's units.

The last material considered for the DFSSs is Teflon. Its dielectric permittivity is the lowest among the considered materials. As shown in the Figure 10 a) and b), the highest wavelength resonance occurs at 1.19. This resonance is very strong and stable for all cases, similar to the Plexiglass cases. The resonance curve exhibits a good quality factor.

In comparison, the dielectric permittivity of Plexiglass is higher than that of Teflon, resulting in a better resonance quality factor. On the other hand, higher dielectric permittivity in the cases of E-Glass and Taconic CER-10 are accompanied by poorer quality factors.

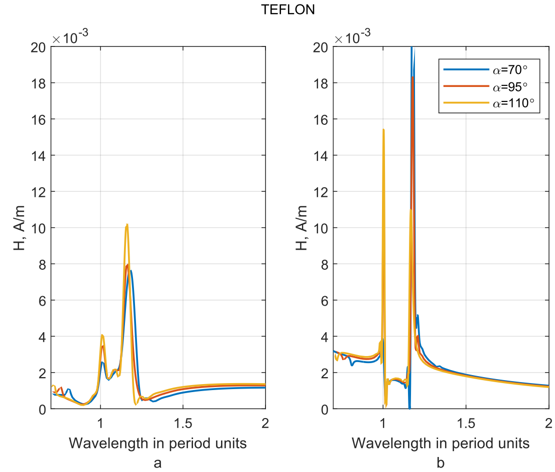

FIGURE 10. Magnetic fields in the test point, Taconic CER-10 case. a) incident wave downward, b) incident wave upward

The different incidence angles should be analyzed in a separate investigation. Here, only cases with small incidence angles are demonstrated. As the Figures 11 and 12 show, at large wavelengths, there are no significant differences in the obtained field configurations compared to normal incidence. However, the differences become apparent at shorter wavelengths.

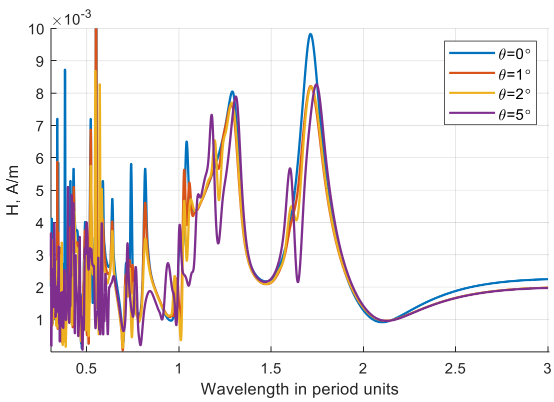

FIGURE 11. Magnetic fields in the test point, for E-Glass and different incidence angles θ.

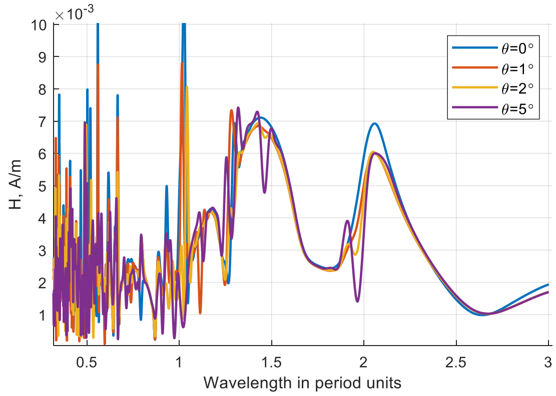

FIGURE 12. Magnetic fields in the test point for Taconic CER-10 and different incidence angles θ.

V. CONCLUSION

This study formulated the magnetic current's periodic Green function and applied it within the MAS framework to solve problems involving p-polarized plane wave incidence on Dielectric Frequency Selective Surfaces (DFSS) and investigated the potential of Dielectric Frequency Selective Surfaces (DFSS) as concentrators of alternating magnetic fields for plasma density control applications. By employing the MAS, DFSSs composed of various dielectric materials, including E-Glass, Plexiglass, Taconic CER-10, and Teflon were analyzed. Numerical simulations revealed several key insights.

It is found that the dielectric permittivity of the material significantly affects the resonance properties and quality factors of DFSSs. Materials with lower dielectric permittivity, such as Plexiglass and Teflon, exhibited higher resonance quality factors. In contrast, higher permittivity materials like E-Glass and Taconic CER-10 showed poorer quality factors.

The geometric configuration of DFSSs plays a crucial role in their performance. The considered profile with periodic "humps" having varied slope angles demonstrated that resonance frequencies remained relatively stable despite geometric variations, which is essential for practical fabrication.

The study highlighted specific resonance frequencies for different materials, with the highest wavelength resonances occurring at 2.054 for Taconic CER-10 and 1.19 for Teflon. These resonances are strong and stable, making DFSSs suitable for applications requiring precise control of magnetic fields and plasma density. The ability of DFSSs to generate strong magnetic fields at resonance frequencies suggests their potential use in enhancing plasma density for industrial processes like thin film deposition.

For small incidence angles in the large wavelength range, the field configuration exhibits smooth behavior. At short wavelengths, an extremely high number of resonances is observed.

Overall, the results of this study demonstrate the feasibility and effectiveness of DFSSs in controlling magnetic fields and plasma density. The insights gained regarding material selection and geometric design provide a foundation for further research and development of advanced dielectric resonators for various industrial applications

ACKNOWLEDGMENT

This work was supported by Shota Rustaveli National Science Foundation (SRNSF) [Grant number: STEM-22-192].

REFERENCES

[1] M. Bozzi, L. Perregrini, "Design, fabrication, and measurement of frequency-selective surfaces", Optical Engineering, Vol. 39 No. 8, 2263- 2269, 2000.
[2] M. Bozzi, L. Perregrini, "Analysis of Multilayered Printed Frequency Selective Surfaces by the MoM/BI-RME Method", IEEE Transactions on Antennas and Propagation, vol. 51, No. 10. 2830-2836, 2003.
[3] H. L. Bertoni, Li-Hsang S. Cheo, T. Tamir, "Frequency-Selective Reflection-Transmission by a Periodic dielectric Layer", IEEE Transactions on Antennas and Propagation, vol. 37, No. 1, 79-83, 1989.
[4] N. L. Tsitsas and C. Valagiannopoulos, "Anomalous refraction into free space with all-dielectric binary metagratings", Physical Review Research 2, 033526, 2020.
[5] A. A. Maradudin, I. Simonsen, J. Polanco, and R. M. Fitzgerald, "Raylegh and Wood anomalies in the diffraction of light from a perfectly conducting reflection grating", J. Opt. 18, 024004, 2016.
[6] J. Bornemann, "Computer-Aided Design of Multilayered Dielectric Frequency-Selective Surfaces for Circularly Polarized Millimeter-Wave Applications", IEEE Transactions on Antennas and Propagation, vol. 41, No. 11, 1588-1591, 1993.
[7] P. Harms, R. Mittra, and K. Wai, "Implementation of the periodic boundary condition in the finite-difference time-domain algorithm for FSS structures", IEEE Trans. Antennas Propagat., vol. 42, pp. 1317–1324, 1994.
[8] M. Lambea, M. A. Gonzalez, J. A. Encinar, and J. Zapata, "Analysis of frequency selective surfaces with arbitrarily shaped apertures by finite element method and generalized scattering matrix", in IEEE APS Int. Symp. pp. 1644–1647, 1995,
[9] R. Mittra, C. H. Chan, and T. Cwik, "Techniques for analyzing frequency selective surfaces — A review", Proc. IEEE, vol. 76, pp. 1593–1615, 1988.
[10] H. Sugai, I. Ghanashev, and M. Nagatsu, "Production and control of large diameter surface wave plasmas", Plasma Sources Sci. Technol. 7, 192, 1998.
[11] A. Iwai, O. Sakai, and Y. Omura, "One-dimensional particle simulation of wave propagation and generation of second harmonic waves in a composite of plasma and metamaterial", Phys. Plasmas 24, 122112, 2017.
[12] W. Rotman, "Plasma simulation by artificial dielectrics and parallel-plate media", IRE Trans. Antennas Propag., 10, 82, 1962.
[13] Kupradze V. "About Approximates Solution Mathematical Physics Problem", Success of Mathematical Sciences, Moscow, 22. N2, pp 59-107, 1967.
[14] G. Kyurkchan, B.Yu.Sternin, V. E. Shatalov, "Singularities of continuation of wave fields", Phys.-Usp. 39 pp.1221-1242, 1996.
[15] R. Zaridze, G. Bit-Babik, K. Tavzarashvili, N. Uzunoglu, and D. Economou, "Wave Field Singularity Aspects Large-Size Scatterers and Inverse Problems", IEEE Transactions on Antennas and Propagation, vol. 50, No. 1. p. 50-58, R, 2002.
[16] J. Lee, S. Nam, "Protecting the method of auxiliary sources (MAS) solutions from the interior resonance problem", IEEE microwave and wireless components letters, vol. 15, no. 3. p 186- 188, 2005.
[17] R.F. Harrington, "Field computation by moment methods", New-York: Macmillan; 1968.
[18] S.M. Rao, D.R. Wilton, and A.W. Glisson, "Electromagnetic scattering by surfaces of arbitrary shape", IEEE Trans Antennas Propag; 30 409–18, 1982.
[19] J. Blackburn and L. R. Arnaut," Numerical Convergence in Periodic Method of Moments Analysis of Frequency-Selective Surfaces Based

on Wire Elements". IEEE Transactions on Antennas and Propagation, vol. 53, No. 10. p. 3308-3315, 2005.

[20] K. Tavzarashvili, Ch. Hafner, Cui Xudong, R. Vahldieck, D. Kakulia, G. Ghvedashvili, and D. Karkashadze," Method of Auxiliary Sources and Model-Based Parameter Estimation for the Computation of Periodic Structures", Journal of Computational and Theoretical Nanoscience, Vol.4, 3, pp.667-674, 2007.

[21] R. W. Ziolkowski and E. Heyman, Phys. Rev. E 64, 056625, 2001.

[22] R. Lampe, P. Klock, P.Mayes, "Integral Transforms Useful for the Accelerated Summation of Periodic, Free-Space Green's Functions", IEEE Transactions on Microwave and Techniques, Vil. MTT-33, No. 8, p 734-736, 1985.

[23] C. Craeye, A. B. Smolders, D. H. Schaubert, and A. G. Tijhuis, "An Efficient Computation Scheme for the Free Space Green's Function of a Two-Dimensional Semiinfinite Phased Array", IEEE Transactions on Antennas and Propagation, vol. 51, No. 4, April, p. 766-771, 2003.

[24] D. Kakulia, K. Tavzarashvili, G. Ghvedashvili, D. Karkashadze, and Ch. Hafner, "The Method of Auxiliary Sources Approach to Modeling of Electromagnetic Field Scattering on Two-Dimensional Periodic Structures", Journal of Computational and Theoretical Nanoscience, Volume 8, pp. 1609-1618(10), 2011.

[25] M. Inoue, "Enhancement of local field by two-dimensional array of dielectric spheres placed on the substrate", Phys. Rev. B, vol. 36 #5, p 2852-2862, 1987.

[26] D. M. Natarov, V.O. Byelobrov, R. Sauleau, T.M. Benson, and A.I. Nosich, "Periodicity-induced effects in the scattering and absorption of light by infinite and finite gratings of circular silver nanowires", Opt. Express, 19 (22), p. 22176-22190, 2011.

[27] C. A. Valagiannopoulos, N. L. Tsitsas, and G. Fikioris, "Convergence analysis and oscillations in the method of fictitious sources applied to dielectric scattering problems", J. Opt. Soc. Am. A, Vol. 29, No. 1 1, 2012.

[28] G. Fikioris, N. L. Tsitsas, and G. K. Charitos, "Spurious oscillations in a combined Method-of-Auxiliary-Sources/Extended-Integral-Equation solution to a simple scattering problem", Journal of Quantitative Spectroscopy & Radiative Transfer, 123 30–40, 2013.